NEW DESIGN OF PLC-BASED ROBOTIC CONTROL SYSTEM FOR CONCRETE PRINTING IN BUILDING CONSTRUCTION

DANIEL KAJZR, JOSEF BROUSEK, TOMAS PETR, LEOS BERAN, MARTIN DIBLIK, ROBERT VOZENILEK

Faculty of Mechatronics, Informatics and Interdisciplinary Studies, Faculty of Mechanical Engineering,

Technical university of Liberec, Liberec, Czech Republic

daniel.kajzr@tul.cz

This paper presents a new platform for the development of an open control system for a robotic arm designed for the 3D printing of buildings. This platform uses a very efficient system of automatic code generation which greatly simplifies the process of robotic arm synthesis and analysis while allowing the deployment of custom control algorithms. An experimental workplace, with a reduced and simplified robotic arm, has been developed for the purpose of testing the platform. The mechanical and electrical construction of this experimental workplace is explained. The control system platform is also introduced and data from the test results are included. Both the advantages and disadvantages are discussed at the end.

KEYWORDS

3D printing, buildings, architecture, robotic arm, cement, concrete

1 INTRODUCTION

Methods for printing buildings using robots are presently being intensively developed. The most commonly used material for printing is concrete. 3D printing, using concrete, has recently received considerable attention. Several reviews have addressed issues relating to 3D printing technology, aspects of the concrete mix and the effective properties of printed concrete [Buswell 2018], [Ngo 2018], [Wolfs 2019], [Shakor 2019], [Wangler 2019], [Khan 2020]. A review of the current state of computerised modelling and simulations in 3D printing of cement-based material is offered in a review article [Khan 2020].

However, key areas are automated systems and robots which enable the printing of these cement mixtures. Currently, the gantry system and modified industrial robots are frequently used for the 3D printing of buildings [Paolini 2019], [Delgado 2019].

Common industrial robots have a number of shortcomings, however, including short-range, high power consumption, the need to stop the entire mechanism in the event of a sharp break in the printed curve, etc. For these reasons, long-range robotic designs are currently being developed which typically mimic common kinematic structures such as Cartesian, Cylindrical, or Spherical. However, such procedures do not solve all of the above problems. One interesting idea for increasing the printing range is the use of a mobile printing system (a manipulator mounted on a mobile base), respectively concurrent 3D printing by multiple mobile robots [Mehmet 2018], [Zhang 2018]. However, such a concept is highly demanding when solving problems relating to motion planning, localization, and motion control.

Article [Zada 2021] contains a set of basic requirements necessary for a robot suitable for 3D printing, which we quote directly here:

i. Since the robot moves the print head mainly in the horizontal position during 3D printing, it is necessary that the robot retains its potential energy as much as possible.

ii. It is also necessary that most of the dynamic effects take place in the horizontal plane, i.e. without the influence of gravity.

iii. Another requirement is, if possible, to maintain kinetic energy in 3D printing. I.e. the need to maintain the movement of most of the robot's links, even if the end tool has to stop for a short time.

iv. Furthermore, the compactness of the robot is important, i.e. the robot can be folded into a relatively small space during transport. Thus, the Cartesian structure is completely unsatisfactory.

v. Because of the dustiness on-site dustiness, it is advisable to use rotating links over sliding ones.

In order to best meet these requirements, a kinematic design, similar to that of the established SCARA structure, has been suggested, but further enhanced with additional parts. The most important of these is the addition of another rotational axis, placed vertically, giving the robot an excessive degree of freedom (DOF) when moving in the horizontal plane (see Figure 1).
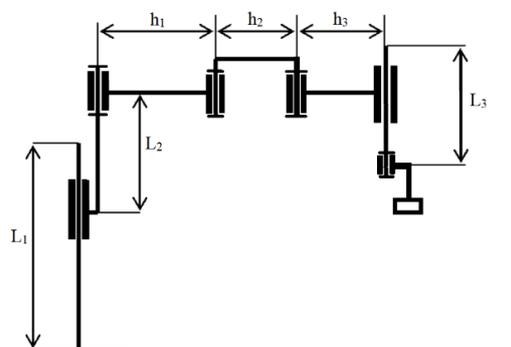
Figure 1. Designed kinematic structure of a robot for 3D printing.

When considering the robotic arm with a non-standard kinematic structure, the question arises how to control such an arm. Nowadays the main requirement for a control system is its openness. The open architecture for robot control allows the extension and modification of its functionality. Several open control architectures have been developed and discussed in publications [Macchelli 2002], [Orocos 2006]. However, their use has remained more within a small group of researchers. These architectures are hardware based on personal computers (PC). The use of PCs for robot control has its advantages and disadvantages. Software development costs are reduced due to the possibility of using high level programming languages. The main disadvantage is that standard computers are not robust and reliable enough for deployment in an industrial environment.

Programmable Logic Controllers (PLC) are typically used as the control device in an industrial environment. PLCs are robust reliable and easy-to-use control systems that are commonly considered as low-level systems. However, modern PLCs have had enough computing power to perform complex mathematical calculations using different programming languages [IEC 2002]. This allows developers to implement various control algorithms and PLC deployments to control robotic systems.

PLC-Based Robotic Controls even represent an interesting alternative to OEM Robotic Controls. Robot original equipment manufacturers (OEMs) offer a tightly integrated controller, but in devices where PLC-based control is already used in other machine control applications, PLC-based robotic control can be an interesting option. This solution will allow the use of one platform for all devices [techbriefs 2015]. Although PLC based robotic control is quite interesting and the current topic, but PLC-based control systems for robotic manipulators are rare and usually limited to simple cartesian or gantry designs [Vojir 2021].

In our article, we want to introduce an open PLC-based control system for a redundant robotic arm. This open control system uses a very efficient way of automatic code generation, which greatly simplifies the process of synthesis, analysis and implementation of robotic system control.

2 NEW ROBOTIC ARM DESIGN

The main aim of this robotic arm design was building an experimental workplace which enabled the development of a control system for the large robotic arm designed for printing cement mixtures. The provisional design of the final robotic arm has a length of 5600 mm. Based on our previous experience in designing robotic arms, we used an effective scale of 1:4 for a small experimental robot. Therefore, the requirement for the length of the experimental robotic arm was 1400 mm. This accuracy of scale allowed us to concentrate on the development of controls for the large robotic arm while, at the same time, the experimental arm was not so demanding on the available workspace. The detailed side layout of the designed experimental robotic arm is shown in Figure 2.

The whole experimental workplace consists of the robotic arm, the robot work table, and the control unit. More detailed information about the workplace can be found in Chapter 4. This chapter focuses on the design of the robotic arm. In addition to the requirements regarding the robotic arm length, it was also necessary to consider the requirements of the arm endpoint in order to be able to trace the endpoint trajectory on the robot work table. Here we can see the results of the controlled path.
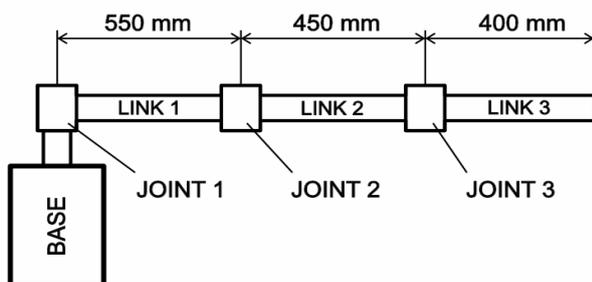
Figure 2. Side layout of robotic arm.

2.1 Mechanical design of experimental robot

Based on the requirements for the length of the individual arms mentioned in the previous chapter, we decided to design an arm structure from laser-cut metal sheet parts. This technical solution enabled us to design a sufficiently rigid arm while guaranteeing a high level availability of local parts at reasonable prices. At the same time, these parts were not particularly high. Therefore, this solution was also advantageous in meeting the requirements regarding the tracing of the endpoint of the arm to the work table. All three links are designed from two facing sheet metal parts. The sheet metal parts of link 1 and link 2 are reinforced with two steel cylinders. Link 1 is also reinforced with an inserted steel rectangular profile. The design for the experimental robotic arm is shown in Figure 3.
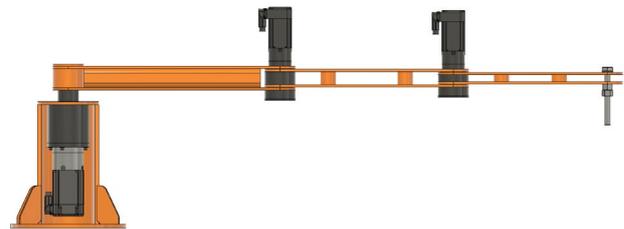
Figure 3. Side view of the experimental robotic arm.

The rotary couplings in joint 2 and joint 3 are formed by sliding cylindrical bearings inserted into holes in the sheet metal parts. The servo flanges in joint 2 and joint 3 are screwed to the sheet metal part of the previous link and the motor shafts are firmly connected by a keyway connection to the cylindrical part of the next link. To increase the rigidity of the joints, a supporting ball bearing is inserted on the underside of the links, ensuring all parts in the joint pull together while, at the same time, allowing the rotation of the two parts. Joint 1 is placed in the base. It consists of two ball bearings housed in a cylinder base, into which the shaft carrying link 1 is inserted. The base consists of a steel cylinder with a sheet metal base which enables the attachment of the robot to the robot work table. Servo driving link 1 is mounted in the base cylinder. The connection to the shaft is also designed using a keyway connection. The two-part table is designed from an aluminium profile system and the table top is made as a whiteboard. Small adjustable legs ensure the levelling and stability of the table. The whole experimental robotic arm with the robot work table is shown in Figure 4. All parts of the robotic arm are connected by screw connections. This solution allows for possible future modifications and ensures easy disassembly in case of the need to transport the equipment, e.g., for exhibitions and presentations.

Figure 4. Experimental robotic arm with robot work table.

2.2 Drive system design

The movement of individual axes is provided by synchronous servomotors with brakes and with planetary gearboxes. Planetary gearboxes are not entirely suitable for use in serial kinematic structures, mainly due to their backlashes. Planetary gearboxes are, however, significantly cheaper than, for example, backlash-free harmonic gearboxes. We were aware of this fact when designing the experimental arm. However, we were mainly focused on controlling algorithms, not on the precision of movement TCP. Therefore, we chose a cheaper and faster variant (considering our time in the project for this design) at the expense of the accuracy of the robotic arm. The first axis is the most dynamically stressed and is driven by a servomotor at a nominal speed of 1500 rpm and a torque of 2.5 Nm. The other two axes are driven by the same servo motors at a nominal speed of 1500 rpm and a torque of 1.330 Nm. The gear ratio of all gearboxes is 40 and the nominal moments are 82 Nm (Axis1) and 30 Nm (Axis2, Axis3). The servo motors are equipped with absolute incremental sensors with the highly advanced interface EnDat 2.2. The detailed drive specifications are shown in Table 1.

Axis1				
synchronous servomotor		planetary gearbox	General values	
Nominal speed [rpm]	1500	Number of gear stages	2	Max. permissible output torque M_{K0} [Nm]	80.5
Nominal torque Mn [Nm]	2.5	Gear ratio i	40	Mass of motor (without brake) [kg]	2.45
Nominal current I_N[A]	6	Nominal output torque T_{2N} [Nm]	82	Mass of gearbox [kg]	2.9
Axis2,3				
synchronous servomotor		planetary gearbox	General values	
Nominal speed [rpm]	1500	Number of gear stages	2	Max. permissible output torque M_{K0} [Nm]	30
Nominal torque Mn [Nm]	1.33	Gear ratio	40	Mass of motor (without brake) [kg]	1.45
Nominal current I_N [A]	3.2	Nominal output torque T_{2N} [Nm]	30	Mass of gearbox [kg]	1.5

Table 1. Drive specifications.

2.3 Control system design

The robotic arm's control system is designed for Simulink, using B&R Automation Studio Target for Simulink [BR 2019], allowing the easy-to-use implementation of the target control system – an Industrial PC.
B&R Automation PC 2100 is used as the target control system. It is an industrial PC based on Intel Bay Trail architecture. It is equipped with a single-core processor – Intel Atom E3815 1.46 GHz, 1 GB SDRAM, and 2 GB CFast SLC cards. The Automation PC 2100 integrates all necessary interfaces, including 2x Gigabit Ethernet as well as 1x USB 2.0 and 1x USB 3.0, and is supplemented by additional interface modules such as RS232, CAN, POWERLINK, X2X Link, which are not necessary for our task.

The electric drives within the individual axes are controlled by a servo drive, B&R Acopos P3, which is connected to the Automation PC via Powerlink. Acopos P3 is a 3-axis servo controller which integrates safety functions, high dynamics, and accuracy with a sampling time of just 50 µs for the entire controller cascade (position controller loop). It has an Endat 2.2 interface for each axis. The nominal current of Acopos is 8.8 A. The block schematic representation of the proposed system is shown in Figure 5.
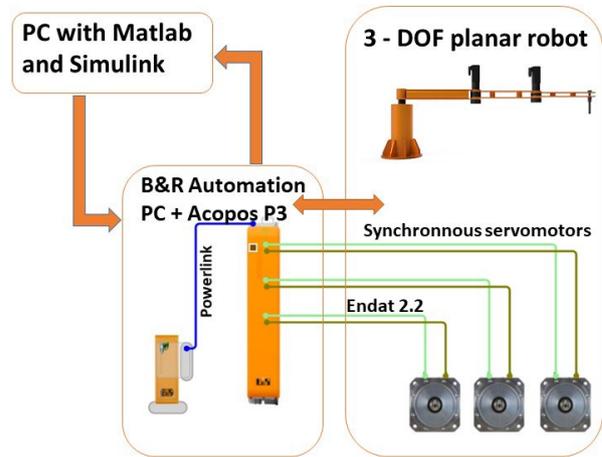
Figure 5. Schematic representation of the proposed system.

3 KINEMATIC MODEL AND WORKING AREA OF EXPERIMENTAL ROBOT

Our experimental robot is a planar manipulator with three degrees of freedom. All joints are rotational with the range of individual axes limited only by the mechanical design. DH parameters of the experimental robot and the range of the individual axis are listed in Table 2.

Axis	Θ	d	a (mm)	Range
1	Θ_1	0	h1 = 550	-180° - 180°
2	Θ_2	0	h2 = 450	-105° - 105°
3	Θ_3	0	h3 = 400	-125° - 125°

Table 2. DH parameters of the experimental robot.

3.1 Kinematic model

The transformation equations of the robot's kinematics are:

$$x(t) = h_1\cos(\Theta_1) + h_2\cos(\Theta_1 + \Theta_2) + h_3\cos(\Theta_1 + \Theta_2 + \Theta_2) \quad (1)$$

$$y(t) = h_1\sin(\Theta_1) + h_2\sin(\Theta_1 + \Theta_2) + h_3\sin(\Theta_1 + \Theta_2 + \Theta_2) \quad (2)$$

where h_1, h_2 and h_3 are the lengths of the link 1,2 and 3 and Θ_1, Θ_2, Θ_3 are joint variables.
The robot's forward kinematic, determined by the coordinates x(t), y(t) at a given point in time from the entered values of Θ_i, is an easy task. The more difficult task is the robot's inverse

kinematic, determined by finding angles (Θ_1, Θ_2, Θ_3) for a given point in coordinates $x(t)$, $y(t)$.

According to Article [Zada 2021] we have several possible solutions here:

 i. choose some variable as a parameter and calculate other variables

 ii. choose a fixed linkage between the angles Θ_1, Θ_2, Θ_3 to get the third equation.

 iii. determine the angles Θ_1, Θ_2, Θ_3 as an extremal problem for the selected optimization criterion.

The complete solution of robot inverse kinematic is in Article [Záda 2021].
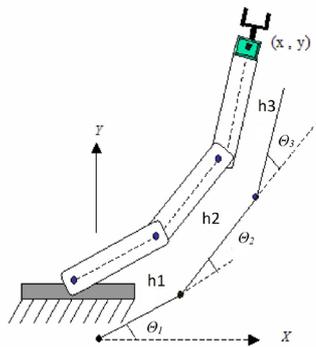
Figure 6. Geometric representation of a 3 DOF planar manipulator at joint angles (Θ_1, Θ_2, Θ_3).

3.2 The working area of experimental robot

If we consider that all axes can rotate about 360°, the workspace would be a simple circle of radius $h_1 + h_2 + h_3$. When some limits exist, the workspace becomes more complicated.

Consider, for example, the first case for solving inverse kinematics and that we chose variable Θ_1 as a parameter, precisely equal to zero. Considering the constraints of axes 2 and 3, the working area of the robotic manipulator will look like Figure 7.
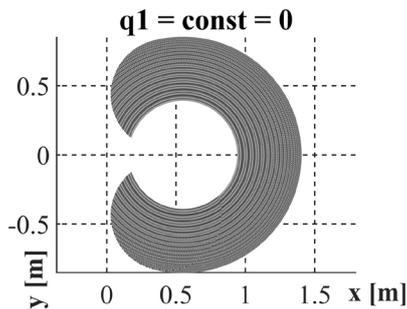
Figure 7. Working space of the 3DOF planar manipulator for the case Θ_1 = const. = 0 with respect to the coordinates (x, y).

By changing the variable Θ_1, the working area will shift. Figure 8 shows the robotic manipulator working area when considering the working range of axis 1 from -180 to 180 degrees.

Figure 8. Whole workspace of planar 3R manipulator including physical limitations relative to the (x, y) coordinates.

4 EXPERIMENTAL WORKPLACE

As already mentioned, our primary goal was building an experimental workplace enabling the development of a control system for the pre-existing large robotic arm designed for printing cement mixtures. The experimental workplace consists of a robotic arm, a work table, and a control unit.

The work table is 1.5 wide × 1.7 m long and serves as a drawing canvas for testing the movement of the endpoint of the robotic arm along the generated trajectories. As an endpoint of a robotic arm - a tool, we used a pen holder, which we modelled and printed it on a 3D printer. Figure 9 shows the developed robotic arm drawing a generated trajectory in the form of a straight line on the desktop. Figure 10 shows the electrical switchboard of the robotic arm and a preview of the control unit.
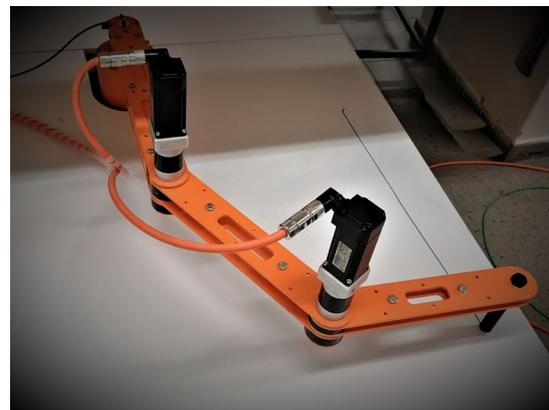
Figure 9. Real experimental robotic arm with robot work table.
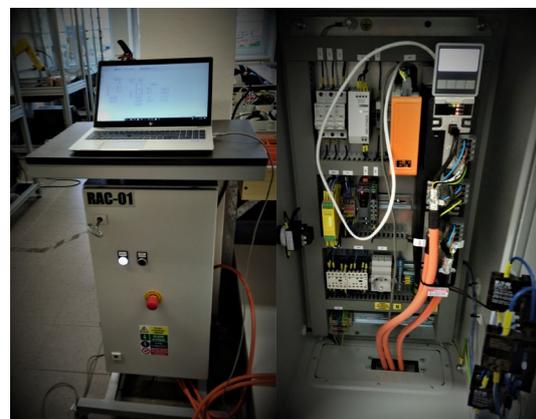
Figure 10. Control unit of experimental robotic arm.

4.1 Software implementation

B&R Automation Studio is used as the developmental environment. B&R Automation Studio is an integrated software development environment that contains tools for all project phases. Control, drive, communication, and visualization can all be configured in one environment, reducing both integration time and maintenance costs [BR 2019].

Automatic code generation is used with the help of the BR Target for the implementation of Simulink models. This complement enables us to easily "transfer" the designed simulation schemes from Simulink to Automation Studio and its subsequent launch on a real PLC. Simulation schemes are automatically transferred by Simulink Coder® or Embedded Coder® into a source code in C/C++ language; therefore, writing the program manually is eliminated [B&R 2019].

The Figure 11 shows the process of implementing control based on models designed in Matlab/Simulink.
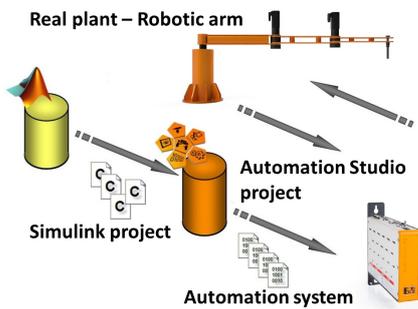
Figure 11. Simulink model based control implementation process.

5 RESULTS

To test the functionality of the developed robotic arm and control system, we generated an endpoint trajectory corresponding to a simplified wall shape with ribbing - "a ribbed trajectory". The trajectory starts at a point with coordinates [x,y] = [1.4, 0] and from zero angles. The time for passing the robot along the given trajectory is about 80 s. In curves, we considered the deceleration of the endpoint velocity from 0.1 m/s to 0.25 m/s. For the selected trajectory, we solved the inverse problem for individual cases described in chapter 3 with the help of Matlab. Figure 12 shows the above mentioned endpoint trajectory "a ribbed trajectory".
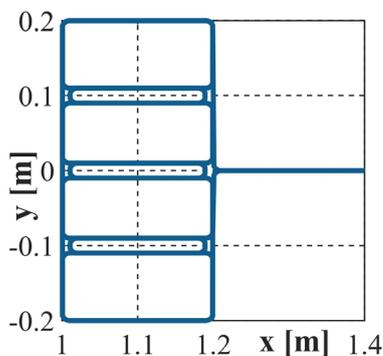
Figure 12. XY Graph of generated trajectory, horizontal axis: x [m], vertical axis: y [m].

In developing a solution for the inverse kinematics problem, we obtained the functions of joint variables for individual axes for

3 cases: Θ_1 = const. = 0, Θ_2 = k x Θ_3 (k = 1) and Θ_2 = k x Θ_3 (k = -1). We used the functions of joint variables as desired positions for position control, and we measured the moments on individual drives. To generate the joint variables' required values, we created a Simulink model with a sampling period of 2ms.

The Figure 13 shows the Simulink model for generating set points of joint variables, supplemented by blocks from the B&R AS Target for Simulink libraries, for the possibility of using automatically generated code for controlling the robotic arm.
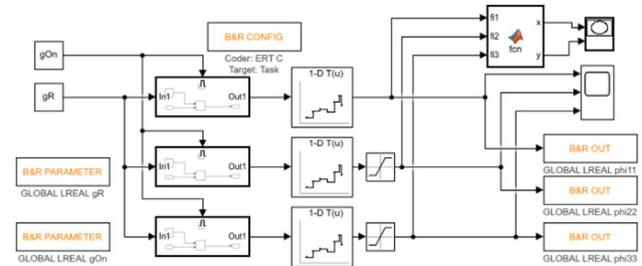
Figure 13. Simulink model for generating set points of joint variables.

The following Figures 14-16 show real measured time behaviours of individual joint angular positions, corresponding angular speeds and measured torques in joints. The individual figures show various possibilities of the solution of inverse kinematics, see chapter 3.1. The reference trajectory is the same for all cases and is shown in the Figure 12.

Figure 14 shows the case where we choose the first joint variable as the parameter Θ_1 = const. = 0. Figures 15 and 16 show the case where we choose a fixed linkage between the joint variables, specifically Θ_2 = k x Θ_3 where k = 1 for Figure 15 and k = -1 for Figure 16. The individual drives' moments correspond to the dynamic load of the robotic arm's individual joints within the given trajectory.
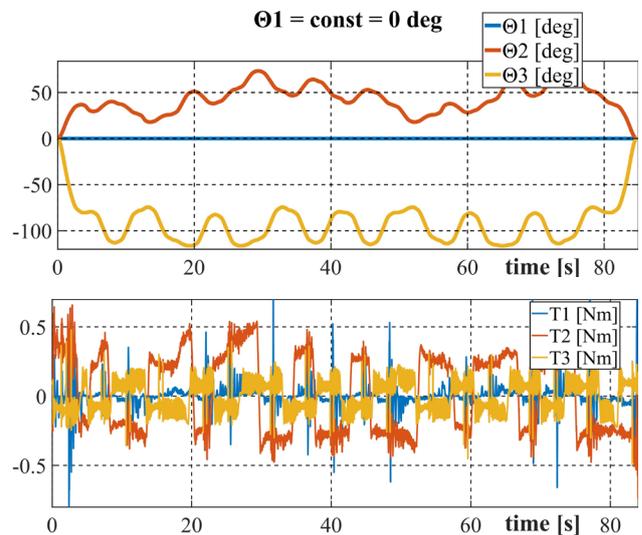
Figure 14. Angular displacement of the joints for a given trajectory, for the case Θ_1 = const. = 0 and the individual drives' corresponding torques.
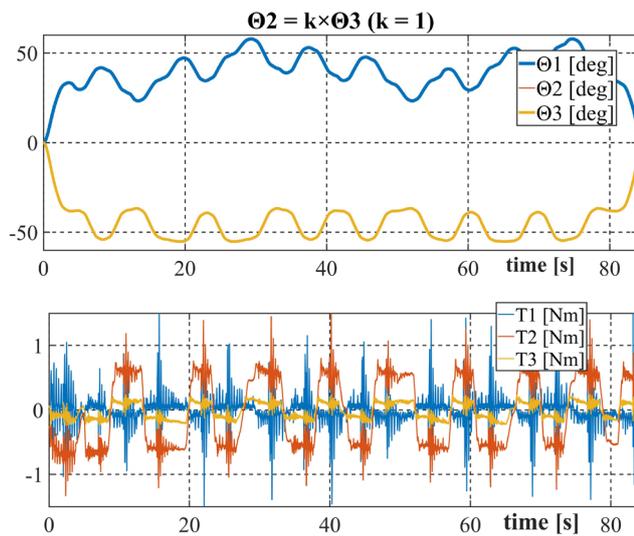
Figure 15. Angular displacement of the joints for a given trajectory, for the case $\Theta2 = k \times \Theta3 \ (k = 1)$ and the individual drives' corresponding torques.
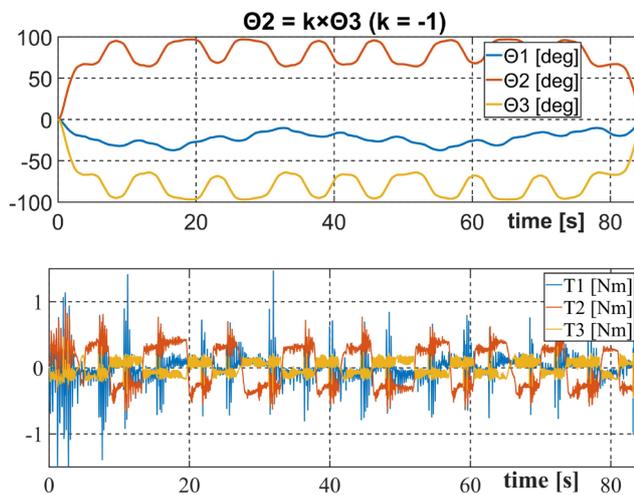
Figure 16. Angular displacement of the joints for a given trajectory, for the case $\Theta2 = k \times \Theta3 \ (k = -1)$ and the individual drives' corresponding torques.

6 CONCLUSIONS

In this paper, we introduced the concept of a PLC-based robotic control system using a very effective method of creating the code for the path controller using B&R AS Target for Simulink. This control system is unique compared to others in that it allows direct use of Matlab for design, analysis, testing and implementation of the control. This can save a lot of time and allows us to deploy the control on a robotic arm of any kinematic structure.

Our experimental workplace fulfilled it's set requirements. We were able to test basic controls for our new kinematic for cement mixtures printing. Our results show it is possible to create a predefined path from an architect. The shape can be both very random and very interesting from the architectural point of view. This is one of the main targets of 3D printing in building construction.

We verified the robotic arm's movement along a trajectory generated by us, corresponding to the wall's simplified shape with ribbing - a ribbed trajectory. We tested three different ways of solving the robotic arm's inverse kinematics and obtained three different combinations of waveform variables

for one endpoint trajectory. We measured the moments on the drives for the given courses of articulated variables. Based on these measurements, the least energy-intensive trajectories, etc. could be selected. As far as the accuracy of the robotic arm's endpoint is concerned, there are clearances in planetary gearboxes and they are not entirely appropriate use of a grooved connection between the motor shafts and the gearboxes.

Our next work will focus on the development of a larger robotic arm, to the scale of 1:2, which will allow for better mechanical parameters. The precision of the arm must be improved to enable its use as a rigid robotic system in the building industry. All electric drives, including gearboxes, will be replaced to have lower or zero backlash in all joints.

REFERENCES

[Buswell 2018], R.A Buswell, W.R. Leal de Silva, S.Z. Jones, J. Dirrenberger, "3D printing using concrete extrusion: a roadmap for research". Loughborough University, Volume 112, Journal contribution, 2018, pp. 37-49, ISSN 0008-8846., doi: 10.1016/j.cemconres.2018.05.006.

[B&R 2019] B&R Industrial Automation, Automation Studio Target for Simulink 293: B&R, 2019.

[Delgado 2019] J. M. D. Delgado, L. Oyedele, A. Ajayi, L. Akanbi, O. Akinade, M. Bilal, H. Owolabi, "Robotics and automated systems in construction: Understanding industry-specific challenges for adoption", Journal of Building Engineering, Volume 26, 2019, 100868, ISSN 2352-7102, doi: 10.1016/j.jobe.2019.100868.

[IEC 2002] I.E.C., "IEC 61131-3. Programmable Controllers - Part 3: Programming Languages (2nd Edition)," Final Draft International Standard (FDIS), 2002

[Khan 2018] M. Khan, "3-D printing in transportation: already in action", TR News, 2018, pp. 20–26, ISSN: 0738-6826.

[Khan 2020] M. Khan, F. Sanchez, H. Zhou. "3-D printing of concrete: Beyond horizons". Cement and Concrete Research. Volume 133, 2020, ISSN 0008-8846, doi: 133. 10.1016/j.cemconres.2020.106070.

[Macchelli 2002] A. Macchelli, C. Melchiorri, "A real-time control system for industrial robots and control applications based on real-time Linux", in 15th IFAC World Congress, Barcelona, Spain, July 2002, pp. 55-60.

[Mehmet 2018] T. Mehmet, Z. Xu, P. Quang Cuong. "Printing-while-moving: a new paradigm for large-scale robotic 3D Printing". International Conference on Intelligent Robots and Systems (IROS), Macau, China, 2019, pp. 2286-2291, doi: 10.1109/IROS40897.2019.8967524

[Ngo 2018] T.D. Ngo, A. Kashani, G. Imbalzano, K.T.Q. Nguyen, D. Hui, "Additive manufacturing (3D printing): a review of materials, methods, applications and challenges," Compos. Part B 143, 2018, pp. 172–196. doi: 10.1016/j.compositesb.2018.02.012.

[Orocos 2006] The Orocos Project, "Open Robot Control Software" [online]. 2006 [cit. 2021-09-06]. Available from:

https:// orocos.org/

[Paolini 2019] A. Paolini, S. Kollmannsberger, E. Rank. "Additive manufacturing in construction: A review on processes, applications, and digital planning methods". Volume 30,

2019, 100894, ISSN 2214-8604, doi: 10.1016/j.addma.2019.100894.

[Shakor 2019] P. Shakor, S. Nejadi, G. Paul, S. Malek," Review of emerging additive manufacturing technologies in 3D printing of cementitious materials in the construction industry", Frontiers in Built Environment 4, 2019. doi: 10.3389/fbuil.2018.00085

[Vojir 2021] Vojir, M. et al. A New Way to Design Software for Industrial Automation – 3d Printer Cement Mixtures. MM Science Journal, March 2021, pp 4223-4229. DOI: 10.17973 /MMSJ.2021_03_2020063

[Wangler 2019] T. Wangler, N. Roussel, F.P. Bos, T.A.M. Salet, R.J. Flatt, "Digital concrete: a review", Cem. Concr. Res. 123, 2019. ement and Concrete Research,

Volume 123, 2019, 105780, ISSN 0008-8846, doi: 10.1016/j.cemconres.2019.105780.

[Wicks 2015] M. Wicks, "PLC-based robotic controls versus OEM robotic controls". Tech Briefs [online]. April, 2015, [cit. 2021-09-06]. Available from: https://www.techbriefs.com/component/content/article/tb/su pplements/mcat/features/articles/21862

[Wolfs 2019] Wolfs, R. J. M., Bos, F. P. "Hardened properties of 3D printed concrete: the influence of process parameters on interlayer adhesion". *Cement and Concrete Research*, *119*, 2019, pp. 132-140. Doi: 10.1016/j.cemconres.2019.02.017

[Wolfs 2019] Wolfs, R. J. M., A. S. J. "Structural failure during extrusion-based 3D printing processes". *International Journal of Advanced Manufacturing Technology*, *104*(1-4), pp. 565-584. doi: 10.1007/s00170-019-03844-6

[Zada 2021] V. Zada, K Belda. "Structure Design and Solution of Kinematics of Robot Manipulator for 3D Concrete Printing" ("Accepted as Regular Paper", submitted: 17. 1. 2021 to the IEEE Transactions on Automation Science and Engineering), DOI: 10.1109/TASE.2021.3133138

[Zhang 2018] X. Zhang, L. Mingyang, L. J. Hui , Y. Weng, Y. D. Tay, H. Pham, Q-C. Pham, "Large-scale 3D printing by a team of mobile robots", Automation in Construction, Volume 95, 2018,

pp. 98-106,ISSN 0926-5805, doi: 10.1016/j.autcon.2018.08.004.

CONTACT:

Ing. Daniel Kajzr
Technical University of Liberec, Faculty of Mechatronics, Informatics and Interdisciplinary Studies Studentska 1402/2, Liberec 1, 461 17, Czech Republic
+420 48535 3510, daniel.kajzr@tul.cz, www.tul.cz